Path Sampling Methods for Enzymatic Quantum Particle Transfer Reactions

M.W. Dzierlenga[1], M.J. Varga[1], S.D. Schwartz[2]
University of Arizona, Tucson, AZ, United States
[2]Corresponding author: e-mail address: sschwartz@email.arizona.edu

Contents

Abstract

The mechanisms of enzymatic reactions are studied via a host of computational techniques. While previous methods have been used successfully, many fail to incorporate the full dynamical properties of enzymatic systems. This can lead to misleading results in cases where enzyme motion plays a significant role in the reaction coordinate, which is especially relevant in particle transfer reactions where nuclear tunneling may occur. In this chapter, we outline previous methods, as well as discuss newly developed dynamical methods to interrogate mechanisms of enzymatic particle transfer reactions. These new methods allow for the calculation of free energy barriers and kinetic isotope effects (KIEs) with the incorporation of quantum effects through centroid molecular dynamics (CMD) and the full complement of enzyme dynamics through transition path sampling (TPS). Recent work, summarized in this chapter, applied the method for calculation of free energy barriers to reaction in lactate dehydrogenase (LDH) and yeast alcohol dehydrogenase (YADH). We found that tunneling plays an insignificant role in YADH but

[1] These authors contributed equally to this work.

Methods in Enzymology
ISSN 0076-6879
http://dx.doi.org/10.1016/bs.mie.2016.05.028

plays a more significant role in LDH, though not dominant over classical transfer. Additionally, we summarize the application of a TPS algorithm for the calculation of reaction rates in tandem with CMD to calculate the primary H/D KIE of YADH from first principles. We found that the computationally obtained KIE is within the margin of error of experimentally determined KIEs and corresponds to the KIE of particle transfer in the enzyme. These methods provide new ways to investigate enzyme mechanism with the inclusion of protein and quantum dynamics.

1. INTRODUCTION

The determination of reaction rates is a crucial cornerstone in the study of enzymatic reaction mechanism. In particular, noting how the rate constant changes with respect to isotopic substitution, called a kinetic isotope effect (KIE), can provide a level of mechanistic detail that is otherwise inaccessible. Reaction rates and KIEs have classically been found using a host of experimental techniques which have some limitations, sometimes leading to ambiguous or confusing results. Experimental determination of KIEs currently relies on three overarching classes of methods: noncompetitive, competitive, and equilibrium perturbation. Noncompetitive methods, also known as direct comparison methods, provide the method for the determination of the KIEs on V itself, in addition to V/K, where V is the maximum rate achieved by the enzyme, and K is the substrate concentration at which the rate is half of V. While this is an advantage over other methods, noncompetitive methods are limited in sensitivity compared to other methods, and thus are mostly useful only for large isotope effects, such as primary H/D effects. Competitive and equilibrium perturbation methods alleviate the sensitivity issues of noncompetitive methods, allowing the determination of effects on the scale of 1–3%, but can only determine the KIE on V/K and require a great deal of care in their experimental setup and execution (Cook & Cleland, 2007).

One important use of KIEs is to provide information about the contribution of nuclear tunneling in enzymatic reactions. The main experimental marker of tunneling in particle transfer reactions is an elevated Swain–Schaad exponent (Cha, Murray, & Klinman, 1989). The Swain–Schaad equation relates the KIE of different isotopes, often H/D to H/T, and has an exponential relationship between the two KIEs (Swain, Stivers, Reuwer, & Schaad, 1958). Using only the masses, one can determine a semiclassical lower limit for the exponent, which disregards tunneling effects

(Swain et al., 1958). Elevation above this semiclassical limit has been used to argue for the presence of nuclear tunneling in transfer reactions (Cha et al., 1989; Saunders, 1985). However, the source of this elevation may also be explained by other factors, such as differences in the enzyme's tunneling ready state structure, ie, the ensemble of active site structures at the point at which the particle tunnels, between the isotopically substituted enzymes (Roston & Kohen, 2013).

These experimental ambiguities necessitate methods which can provide complimentary detail while circumventing their limitations. This is the role of computational methods in the study of enzymatic reaction mechanisms. These methods provide the atomistic detail to clarify ambiguous results and to simplify the study of complex systems. For example, the atomistic detail provided by molecular dynamics (MD) simulations allows one to examine the effects on and by individual atoms as opposed to the bulk average effects usually obtained through experimental techniques. Additionally, alteration in the structure, such as through amino acid point mutations or isotopic substitutions, can be performed with relative ease in most of the popular molecular mechanics software packages. Computational methods have the ability to apply these advantages to large enzymatic systems while being able to predict experimental results.

One main computational tool is the calculation of free energy differences between the different states through which the reaction progresses. These free energy differences can be then used to distinguish between different paths the reaction has the ability to pass through, intuit the effects of quantum dynamics, or, through the use of the transition state theory (TST), calculate the rate of reaction. In the following section, we outline some of the most commonly used computational techniques to obtain changes in free energy, reaction rates, and KIEs, along with some of their limitations. Following the introduction of these well-known methods, we detail dynamical methods which can avoid some of these limitations. These dynamical methods are especially suited for the calculation of KIEs and other comparisons between similar enzymatic systems.

1.1 Established Methods for Computational Calculation of Enzymatic Free Energy Barriers and Rates

One method for calculating the free energy barrier of any transition is to find the potential of mean force (PMF) (Kirkwood, 1935, 1936; Onsager, 1933). The PMF, $F(\xi) = -\beta \ln Q(\xi)$, where, β is $(kT)^{-1}$ throughout this chapter,

ξ is the reaction coordinate, and $Q(\xi)$ is the canonical partition function as a function of the reaction coordinate, provides the free energy change for a trajectory obtained by Monte Carlo or MD simulations. For a reaction with low free energy barriers, those on the order of kT, a standard MD simulation will be able to sample the region of interest in a reasonable timeframe and the free energy can be obtained. Of course, most transitions of interest, including most chemical reactions, have barriers much higher than this, which will not be properly sampled by MD simulations without special methods to study rare events.

One such method for the study of rare events is umbrella sampling (Kästner, 2011; Torrie & Valleau, 1977). This method uses a biasing potential to force the system to sample all the regions of interest, even the relatively high energy regions between meta-stable states. In umbrella sampling, the transition is parameterized by a prechosen reaction coordinate and the average force is calculated, via separate simulations, at a variety of reaction coordinate values using the biasing potential. These separate simulations can then be combined and the change in free energy relative to a reference structure obtained by subtracting the biasing potential from the obtained free energy of the windows. Alternate methods to combine windows and obtain a free energy include umbrella integration (Kästner & Thiel, 2005) and the weighted histogram analysis method (Kumar, Rosenberg, Bouzida, Swendsen, & Kollman, 1992).

Umbrella sampling has a long history of successful use but uses a few approximations that can be inappropriate in certain systems. For example, the reaction coordinate must be known, or more usually assumed, in order to bias the system along it. For very simple processes, eg, the movement of a solute through the surface between two immiscible liquids, this may be easy; the distance of the molecule from the surface may be an appropriate reaction coordinate. However, for complex transitions, including all but the simplest chemical reactions, the reaction coordinate is almost impossible to predict a priori. Using chemical intuition, one can create an order parameter that denotes how the system moves along the transition of interest, but all the parts of the reaction coordinate that are not included in the biasing potential are averaged over in the calculation. This reduces the accuracy of the result, and, if the motions not included in the estimated reaction coordinate are important, possibly even an incorrect or misleading result. This issue can be especially prevalent in enzymatic reactions, where many studies have shown that protein dynamics plays a significant enough role in the reaction that it would be difficult to guess without using a method to interrogate the

protein directly (Antoniou, Ge, Schramm, & Schwartz, 2012; Basner & Schwartz, 2005; Crehuet & Field, 2007; Kipp, Silva, & Schramm, 2011; Quaytman & Schwartz, 2007; Silva, Murkin, & Schramm, 2011).

Even if the reaction coordinate is chosen correctly, the umbrella sampling methodology includes the implicit proposal that the motion along the reaction coordinate and the motion along all the other coordinates in the system are completely separable. This is the equilibrium solvation limit from Grote–Hynes theory (Hynes, 1985). In solution phase reactions, this may be an acceptable assumption, but in enzymatic reactions, there is the possibility of protein motions that are correlated to the reaction coordinate and also on the same timescale as barrier crossing. In cases where this type of motion may be important, eg, in enzymatic systems where there may be a promoting vibration, it is not appropriate to average over these motions and doing so affects the accuracy of the results.

In addition to umbrella sampling, there are many other methods to obtain the PMF. These include thermodynamic integration (Straatsma & Berendsen, 1988), also known as blue moon sampling (Ciccotti, Kapral, & Vanden-Eijnden, 2005), and steered MD (Park & Schulten, 2004). Free energy perturbation (FEP) methods are also used, which differ from umbrella sampling and steered MD in that the system is immediately biased to the product state (Zhang, Liu, & Yang, 2000). FEP methods rely on Jarzynski's equality, $\Delta F = -\beta^{-1} \ln \exp(-\beta W)$, where ΔF is the change in free energy, W is the total work performed on the system, and the $\langle \dots \rangle$ denote an ensemble average, to determine the free energy (Jarzynski, 1997).

Free energy methods are often used within the context of the TST to obtain the rates of reaction. TST is a framework which allows for the computation of the rate of transition between two areas of phase space and was first suggested by Horiuti (1938). The rate of reaction from TST is

$$\nu_S^{\mathrm{TST}} = \sqrt{\frac{2}{\pi\beta}} Q^{-1} \int_S e^{-\beta V(x)} \mathrm{d}\sigma(x), \tag{1}$$

where ν_S^{TST} is the rate with dividing surface S, Q is the partition function of reactants, $V(x)$ is the potential energy, and $\mathrm{d}\sigma(x)$ is the surface element on S (Vanden-Eijnden & Tal, 2005). As the TST equation relies on the knowledge of the free energy, it inherits any problems that arise in the free energy calculation. Another issue is that calculation of a KIE involves the combination of two separate rate calculations resulting in a large error in the KIE if one of the rate calculations has a large error. This issue has previously

been considered by Major and Gao (2007), who circumvented the issue by utilizing a mass perturbation approach in an umbrella sampling methodology which determines the KIE in a single calculation.

2. TRANSITION PATH SAMPLING: A NEW PARADIGM FOR THE STUDY OF ENZYMATIC MECHANISM

While the previously outlined techniques are limited in that they map complex dynamical problems onto static approximations, the transition path sampling (TPS) method was developed to study the dynamics of rare events, such as enzymatic reactions, without these approximations (Bolhuis, Dellago, & Chandler, 1998; Dellago, Bolhuis, & Chandler, 1998, 1999; Dellago, Bolhuis, Csajka, & Chandler, 1998). TPS is a dynamical, Monte Carlo technique which samples reactive trajectory space. As TPS is a dynamical method, it allows for the study of systems without a priori knowledge of a reaction coordinate, making it particularly useful for high-dimensional systems such as enzymes.

2.1 A Statistical Method for Studying Enzymatic Reactions

Assume the existence of a two state system, with states R and P, reactants and products in a chemical reaction, or any two meta-stable states. If the typical equilibrium fluctuations of the system do not kick the system out of either state, then the states are stable and long-lived and transitions between the two are rare. This transition can be described by an order parameter, which need not be the exact reaction coordinate, but merely some metric by which the transition can be parameterized. An initial reactive trajectory is obtained, typically by implementing harmonic constraints between donor and acceptor, in transfer reactions, but other methods can be used. From this initial reactive trajectory, a random timeslice is chosen, with momenta p and coordinates q. The momenta at this timeslice are then perturbed randomly, in accordance with a Boltzmann distribution, to create a new set of momenta applied to the original coordinates, which are then propagated forward and backward in time to create a new trajectory. This new trajectory is accepted or rejected via the Metropolis criterion (Bolhuis, Chandler, Dellago, & Geissler, 2002). In a canonical ensemble, the acceptance probability for a new trajectory n, generated from an old trajectory o, is $P_{\text{acc}}^{o\to n} = \min\left(1, \exp\left\{-\beta\left[\mathcal{H}\left(x_0^n\right) - \mathcal{H}\left(x_0^o\right)\right]\right\} h_{\text{R}}\left(x_0^n\right) H_{\text{P}}\left(x_0^n\right)\right)$, where h_{R} and H_{P} are Heaviside functions for commitment to the reactant and visitation

to the product well, respectively. In a microcanonical ensemble, where the system energy is fixed, this acceptance probability simplifies to $P_{\text{acc}}^{o\to n} = h_{\text{R}}\left(x_0^n\right) H_{\text{P}}\left(x_0^n\right))$, which is unity if the trajectory starts in the reactant well and ends in the product well and zero otherwise (Bolhuis et al., 1998). Most uses of TPS in enzymatic systems utilize microcanonical TPS (Dzierlenga, Antoniou, & Schwartz, 2015; Masterson & Schwartz, 2013, 2014). If the new trajectory is rejected, the process is repeated from the last accepted trajectory, but if the new trajectory is rejected, the process continues from the new trajectory. By iteratively adding trajectories to this ensemble, with each new trajectory created with a slice from the previous reactive trajectory, a reactive trajectory ensemble which spans all energetically available paths from reactants to products is created.

TPS only provides an algorithm with which to sample trajectory space and needs a potential energy method to simulate the system in question. In theory, any method can be used, but within the context of particle transfer reactions, quantum mechanics/molecular mechanics (QM/MM) (Warshel & Levitt, 1976) is the most oft used method. A quantum mechanical portion is important in the study of these particle transfer reactions because classical MD methods do not allow for structural changes in chemical bonds, a critical component for any chemical reaction. In particular, the techniques described herein utilize the MD package Chemistry at Harvard Molecular Dynamics (CHARMM) (Brooks et al., 1983, 2009) with a semiempirical quantum region, a PM3 method (Stewart, 1989a, 1989b) modified to better replicate biological zinc (Brothers, Suarez, Deerfield, & Merz, 2004), linked together using the generalized hybrid orbital (GHO) method (Gao, Amara, Alhambra, & Field, 1998). The GHO method provides a well-defined potential energy surface for hybrid QM/MM systems by placing hybrid orbitals on atoms on the QM/MM boundary region, providing better modeling at the QM/MM barrier.

Beyond this flexibility in the choice of force field, TPS can also be used with a variety of propagation methods. One recent development has been the use of normal mode centroid molecular dynamics (CMD) (Cao & Voth, 1994a, 1994b, 1994c, 1994d, 1994e) to include approximate quantum effects in the propagation of the transferring particle in TPS simulations (Antoniou & Schwartz, 2009; Dzierlenga et al., 2015). Full descriptions of the inclusion of this method into TPS can be found in Antoniou and Schwartz (2009), and a short description of this method follows. Each quantum particle is described by a ring of beads connected by harmonic

potentials. The motion of quantum particle i is described by the motion of the centroid of the beads, which is propagated according to

$$m_i \ddot{\boldsymbol{R}}_i = \langle \boldsymbol{F}_i(\boldsymbol{R}_i, \ldots, \boldsymbol{R}_N) \rangle_c, \tag{2}$$

where m_i is the mass of the particle, $\boldsymbol{R}_i$ is the centroid position, $\boldsymbol{F}_i$ is the force on the centroid, and the angle brackets denote a path integral average. This path integral average is weighted by a factor of $\exp(-\beta V_{\text{eff}})$ where V_{eff} is the effective bead potential,

$$V_{\text{eff}}\left(\boldsymbol{r}_i^{\beta}\right) = \sum_{i=1} \sum_{\beta=i} \left[\frac{1}{2} k_i \left(r_i^{\beta} - r_i^{\beta+1} \right)^2 + \frac{1}{B} V\left(r_i^{\beta} \right) \right], \tag{3}$$

A normal mode transformation is applied to separate faster motions of the bead from the relatively slower motion of the centroid (Eq. 4). The effective potential then becomes,

$$V_{\text{eff}}\left(\boldsymbol{R}_i; \boldsymbol{q}_{\alpha}^{i}\right) = \sum_{i=1}^{N} \sum_{\beta=i}^{B-1} \left[\frac{1}{2} m_{\alpha}^{i} \left(\omega_{\alpha}^{i} \boldsymbol{q}_{\alpha}^{i} \right)^2 + \frac{1}{B} V\left(\boldsymbol{R}_i; \boldsymbol{q}_{\alpha}^{i} \right) \right], \tag{4}$$

In addition to separating the motions into two timescales, this transformation allows for the path integral average force to be replaced by the instantaneous force of the propagation of the centroid. Within TPS, this requires a multistep propagation; during the energy calculation at each timestep, the CMD code calculates the force of the quantum particle over several shorter bead propagation timesteps, and this then replaces the CHARMM calculated force of the quantum particle. It should be noted that though CMD allows for the approximate inclusion of quantum effects on the transferring particle, it does so at the price of increased computation time.

2.2 TPS Ensemble Analysis

Examination of the TPS ensemble directly, without the use of additional analysis methods, can provide several types of useful information. One common piece of information gathered from these raw ensembles are distances, often donor–acceptor or transferring particle-donor or -acceptor distances (Dzierlenga et al., 2015). These distances are useful to determine timescales of the reaction, such as the timescale of the transfer event itself, as well as to shed light on timing of the motion of the active site and other nearby residues.

In addition to straightforward examinations of the TPS ensemble, there are also methods which analyze ensembles of trajectories to provide extended detail on the reaction mechanism. One of these methods is the calculation of the committor, which allows for a strict determination of the progress of the reaction more rigorously than a geometrically defined order parameter. This methodology was first developed to study ion-pair recombination (Onsager, 1938) and then repurposed to examine TPS ensembles (Bolhuis et al., 2002). To determine the commitment probability at a point in the trajectory, a series of new trajectories are initiated with random momenta from that point in configuration space. After some period of time, each new trajectory is checked for whether it is in the reactant or product region of configuration space. The fraction of trajectories that have ended in the product region is called the commitment probability, and the point at which the commitment probability is equal to one-half is defined as the transition state. At the transition state, there is an equal probability of proceeding to either the reactants or the products. The set of transition states for a TPS ensemble lies along the transition state surface for the reaction, which is called the separatrix (Bolhuis et al., 2002).

Once a set of several transition states is obtained for a TPS ensemble, committor distribution analysis can be used to determine which motions in the system play significant roles in the reaction coordinate. For this analysis technique, constrained dynamics is begun from a transition state. If the constrained residues are a good approximation of the true reaction coordinate, then the constrained dynamics will travel along the separatrix and will be restricted from alternative motion. Then, the commitment probability is sampled along the constrained dynamics trajectory. After obtaining a distribution of committors via constrained dynamics from a number of transition states with a given reaction coordinate, the distribution of committors is analyzed. If the reaction coordinate constrained during dynamics was close to the true reaction coordinate, the structure during dynamics stayed close to the transition state surface, and the distribution of committors will be sharply peaked about one-half commitment probability. If the presumed reaction coordinate does not accurately account for the true reaction coordinate, then the dynamic trajectories will quickly fall off of the transition state surface and the graph of the committor distribution will not peak at 0.5.

Another technique to analyze the trajectories in a TPS ensemble is essential dynamics (ED), also called principal component analysis (Amadei, Linssen, & Berendsen, 1993). ED was developed to separate the protein degrees of freedom that are constrained from the protein motions that are

able to undergo coherent conformational shifts during dynamics. This is done by first diagonalizing the covariance matrix. Then the resulting eigenvectors can be grouped by their eigenvalues into a small set that contains the coherent conformational changes the protein undergoes, and a set containing the protein degrees of freedom that change little during dynamics. This is a useful tool for the analysis of protein dynamics because it substantially decreases the dimensionality of obtained data, sifting out the degrees of freedom that are essentially constrained during the trajectory.

3. NEW METHODS FOR CALCULATION OF VALUES RELEVANT TO ENZYME MECHANISM

3.1 Free Energy Probes of Nuclear Tunneling

Nuclear tunneling in enzymatic reactions, especially in reactions involving hydrogen transfer where the particle is small enough to often have a significant tunneling contribution, is of interest to those who are involved in determining the mechanisms of enzymes. This is partly because the involvement of nuclear quantum dynamics has been historically neglected from the study of enzyme mechanism (Cha et al., 1989).

To examine the effects of quantum dynamics in enzymatic reactions computationally, we devised a method to examine microscopic free energy changes with respect to the transferring particle that happen along the course of the reaction. By integrating the force on the transferring particle, we obtain the work on the transferring particle from the other atoms in the system. The average of this change in reversible work is the free energy for this step in the reaction in the reference frame of the particle. It is important to note that this free energy change is not the free energy for the entire reaction or for the chemical step of the reaction, but only the free energy change for the transfer of the particle between atoms in the reactive conformation. The probability of a particle to tunnel through a barrier is related to both the height and the width of the barrier. It is not the free energy barrier of the full reaction that is relevant to particle tunneling, but the barrier that exists as the particle transfers, which can be found through the calculation of the work done on the particle.

Unfortunately, a simple integration over the particle path is not sufficient for the barrier to be fully exposed. Even during the particle transfer, the particle does not move directly between the donor and acceptor but also moves against the sides of the potential pocket. To extract the reactive motion from the extraneous motions, a number of steps are taken. The first is to

project the motion of the transferring particle onto the donor–acceptor axis. Since the particle is transferring between these two particles, almost all the reactive motion of the transferring particle will be along this axis. The second is to transform the coordinates of the system such that the hydride work is not affected by the slight movement or rotation of the active site within the protein. This is done by transforming the coordinates so that the donor carbon is at the origin.

The calculation of free energy barriers in this way is useful because it allows for a comparison of the barrier to particle transfer in TPS ensembles. However, when using the method, one must resist the temptation to draw larger conclusions from the method than are appropriate. For instance, putting a free energy obtained from this method into the TST formalism and using it to calculate a rate of reaction would be incorrect, because the free energy calculated using this method is explicitly a free energy difference for the transfer of the particle of interest, not a free energy that corresponds to the full energy barrier for the reaction. However, if one is interested in the barrier to particle transfer to investigate tunneling or to compare two ensembles where the difference is expected to be almost exclusively in the particle transfer, for example, a KIE, then the method is appropriate.

3.1.1 Application of Work Calculation to Hydride Transfer

The calculation of free energy from the work during particle transfer was applied to yeast alcohol dehydrogenase (YADH) and human heart lactate dehydrogenase (LDH) to test for hydride tunneling in these systems. YADH has a long history of use as a model enzyme in research (Ganzhorn, Green, Hershey, Gould, & Plapp, 1987; Hayes & Velick, 1954; Klinman, 1972) and was one of the first enzymes to be used in probes of nuclear tunneling in enzymatic reactions (Klinman, 1976). The seminal study which began to highlight the importance of nuclear tunneling in enzymes used mixed labeling in a competitive experiment to obtain the Swain–Schaad exponents in YADH (Cha et al., 1989). When this exponent was found to be above the semiclassical value, they hypothesized that hydride tunneling played a significant role in the reaction. Nuclear quantum dynamics have subsequently been suspected to play a role in several other enzymatic reactions, including liver alcohol dehydrogenase, soybean lipoxygenase, copper amine oxidase, and others (Klinman, 2009; Layfield & Hammes-Schiffer, 2014; Machleder, Pineda, & Schwartz, 2010; Truhlar, 2010).

Swain–Schaad exponents are a relatively indirect method of addressing questions of quantum dynamics, and competitive labeling experiments

can be muddled due to issues of kinetic complexity, as mentioned previously. To further investigate the issue, we used the free energy barrier calculation from the work of particle transfer to examine tunneling in this enzyme from a different perspective. To determine the contribution of tunneling, we created TPS ensembles with different propagation schemes: an ensemble using a traditional semiempirical QM/MM method that cannot capture nuclear tunneling effects, called the classical ensemble, and an ensemble applying the CMD method to the transferring particle to include these effects, called the CMD1 ensemble. By comparing the free energy barriers between the two ensembles, we were able to deduce the role of tunneling effects in the enzyme. In addition to these two ensembles, we also obtained an ensemble with CMD applied to three particles, the transferring hydride and the other hydrogen atoms bonded to the donor and acceptor carbon, called the CMD3 ensemble. This was done in order to see if there is quantum coupling between the hydrogen in the secondary position and the transferring particle. We also generated an ensemble with CMD applied to only the transferring particle which was substituted for a deuteride, called the CMD-D ensemble, to estimate the primary KIE value in the enzyme.

As can be seen in Table 1, the average value for the classical ensemble is very low; low enough that tunneling is not necessary for reaction. This is further corroborated by the difference between the classical and CMD1 ensemble, which is a difference that is more in line with the inclusion of zero-point energy in the CMD1 ensemble than to tunneling effects. Further evidence for the lack of tunneling is the nonsignificant difference in the distance between the minimum donor and acceptor distance. If tunneling played a major role in the reaction, then one would expect that in the ensembles with quantum dynamics, tunneling would allow for an increase

Table 1 Average Properties of TPS Ensembles with Different Propagation Schemes for the Reaction Catalyzed by YADH

Method	Free Energy Barrier (kcal/mol)	D–A Distance[a] (Å)
Classical	0.97	2.78 ± 0.06
CMD[b]	0.28	2.72 ± 0.09
CMD3[c]	0.32	2.69 ± 0.27
CMD-D[d]	1.05	2.70 ± 0.04

[a]Average minimum in the D–A distance near the reaction.
[b]CMD applied to the transferring hydride.
[c]CMD applied to the secondary hydrogens as well as the transferring hydride.
[d]CMD applied to the transferring deuteride which replaces the hydride in the reaction.

in the donor–acceptor distance by allowing for larger barriers to be surmounted. However, we found no significant difference between the barriers in the CMD1 and CMD3 ensembles. This indicates that quantum coupling between the three hydrogen is not playing a significant role, at least in the energy required for hydride transfer.

In order to compare with an experimental measure, we used the experimental primary H/D KIE to find an energy barrier difference between the two isotopes, under the approximation that the isotopic substitution affects only the free energy barrier, which we then compared to the energy difference of the CMD1 ensemble and CMD-D ensemble. We found that the experimental measured primary deuterium KIE, 3.4 (Klinman, 1976), corresponded to an energy difference of 0.73 kcal/mol, while the difference between our ensembles is 0.77 kcal/mol, a surprisingly close comparison.

In LDH, two different TPS ensembles were generated, one without quantum dynamical propagation, called the classical ensemble, and one with CMD applied to the transferring proton and hydride, called the CMD ensemble. In LDH, unlike in YADH, the proton and hydride transfer at approximately the same time and must both be included in the reaction. The results of the free energy barrier calculation in LDH, shown in Table 2, are somewhat higher than in YADH. The classical barrier was found to be within the range of energies where tunneling can play a role, though it is relatively low. Further evidence that quantum tunneling plays a role in LDH is found in the average donor–acceptor distance, which is significantly lower in the classical ensemble than in the CMD ensemble. This is what one would expect in a situation where tunneling plays a role in the reaction, in that quantum effects allow the particle transfer to occur over a longer distance. It is important to note that the free energy difference has a large range between trajectories within an ensemble, due to the sensitivity to small differences in the trajectories. The distribution of transfer barriers is shown in Fig. 1.

Table 2 Average Properties of TPS Ensembles with Different Propagation Schemes for the Reaction Catalyzed by LDH

Method	Free Energy Barrier (kcal/mol)	D–A Distance[a] (Å)
Classical	7.77	2.77 ± 0.02
CMD[b]	3.61	2.85 ± 0.03

[a]Average minimum in the D–A distance near the reaction.
[b]CMD applied to the transferring hydride and transferring proton.

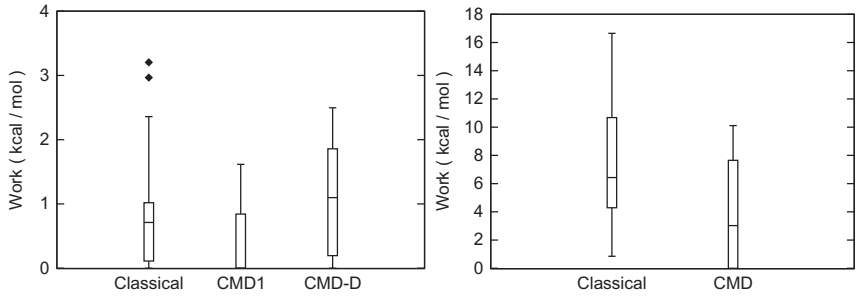

Fig. 1 *Box* and *whiskers plots* made from the barriers to reaction in YADH (*left*) and LDH (*right*). The *center line* marks the median; the *upper* and *lower* ends *of the box* mark the first and third quartiles; the *whiskers* mark the last datum inside the 1.5 times the interquartile range; outside this range, data are marked by *solid squares*.

3.2 KIEs of Quantum Particle Transfer from TPS

In recent work, we developed a method to calculate KIEs from first principle path sampling calculations (Varga & Schwartz, 2016). As in the earlier described study, TPS and CMD were utilized to circumvent limitations of other techniques dealing with the transfer of quantum particles. These methods, combined with an algorithm developed by the Chandler group (Dellago, Bolhuis, &, Chandler, 1998; Dellago et al., 1999; Dellago, Bolhuis, Csajka, et al., 1998), provide a powerful technique for the calculation of KIEs of enzymatic quantum particle transfer reactions.

3.2.1 Rate Calculation Algorithm

Formulation of the rate calculation algorithm starts from a foundation of Bennett–Chandler theory relating the rate of transition between two metastable states to a correlation function (Bennett, 1977; Chandler, 1978). The time derivative of this correlation function, $C(t)$, is the reaction rate constant in the region in which the time derivative of $C(t)$ plateaus, ie, in the steady state. $C(t)$ can be calculated directly with ensemble averages of Heaviside functions for the reactant and product wells, h_r and h_p (Eq. 5)

$$C(t) = \frac{\langle h_{\mathrm{R}}(0) h_{\mathrm{P}}(t) \rangle}{\langle h_{\mathrm{R}}(0) \rangle}. \tag{5}$$

Factorization of $C(t)$ splits the equation into two terms (Eq. 6), where $\langle h_{\mathrm{P}}(t) \rangle_{\mathrm{RP}}$ and $\langle h_{\mathrm{P}}(t') \rangle_{\mathrm{RP}}$ are the ensemble average values of $h_{\mathrm{P}}(t)$ and $h_{\mathrm{P}}(t')$ in the ensemble $F_{\mathrm{RP}}(x_0, T) \equiv \rho(x_0) h_{\mathrm{R}}(x_0) H_{\mathrm{P}}(x_0, T)$, with $H_{\mathrm{P}}(x_0, T)$

denoting trajectories which visit the product well in the interval $[0:T]$. $C(t')$ is a correlation function at a specific time t' in the interval $[0:t)$.

$$k(t) = \frac{\mathrm{d}}{\mathrm{d}t} C(t) = \frac{\left\langle \dot{h_{\mathrm{P}}}(t) \right\rangle_{\mathrm{RP}}}{\left\langle h_{\mathrm{P}}(t') \right\rangle_{\mathrm{RP}}} \times C(t') \tag{6}$$

Thus, the computationally intensive process of calculating $C(t)$ directly at every time t has been simplified to two smaller, more manageable calculations: the calculation of the first term, $h_p(t)$, via one TPS simulation to a plateau region, and the calculation of $C(t')$ via the method described later.

The calculation of $C(t')$ requires a more intensive calculation than the first term. For trajectories starting in the reactant region, R, at time $t = 0$, the distribution of the order parameter, λ, at time t is,

$$P(\lambda, t) = \frac{\int \mathrm{d}x_0 \rho(x_0) h_{\mathrm{R}}(x_0) \delta[\lambda - \lambda(x_t)]}{\int \mathrm{d}x_0 \rho(x_0) h_{\mathrm{R}}(x_0)}. \tag{7}$$

In a rare event system, this distribution is small in the product region, and direct calculation is not feasible. To avoid this difficult, direct calculation, we first define a series of overlapping windows $W[i]$, where $x \in W[i] \rightarrow \lambda_{\min}[i] \leq \lambda(x) \leq \lambda_{\max}[i]$ and the union of all windows $W[i]$ yields the entirety of phase space. The distribution of the order parameter in the windows $W[i]$ is then calculated separately,

$$P(\lambda, t; i) = \frac{\int \mathrm{d}x_0 \rho(x_0) h_{\mathrm{R}}(x_0) h_{W[i]}(x_t) \delta[\lambda - \lambda(x_t)]}{\int \mathrm{d}x_0 \rho(x_0) h_{\mathrm{R}}(x_0) h_{W[i]}(x_t)}. \tag{8}$$

By matching these separate distribution functions, using the overlap windows of each window, where available, we can obtain the full distribution function, $P(\lambda, t)$. The correlation function above, $C(t')$, is then calculated by integration of the product region of this full histogram (Eq. 9).

$$C(t') = \int_{\lambda_{\min}}^{\lambda_{\max}} \mathrm{d}\lambda \, P(\lambda, t) \tag{9}$$

By multiplying these two terms, $\left\langle \dot{h_{\mathrm{P}}}(t) \right\rangle_{\mathrm{RP}} / \left\langle h_{\mathrm{P}}(t') \right\rangle_{\mathrm{RP}}$ and $C(t')$, the reaction rate constant can then be determined. This method has previously been used to determine the rate of reaction in small systems, such as the

dissociation of sodium chloride at air–water (Wick, 2009) and organic-aqueous (Wick & Dang, 2010) interfaces, and to determine the contribution of mechanical stress in the base-catalyzed hydrolysis of tetraglycine (Xia, Bronowska, Cheng, & Gräter, 2011).

3.2.2 Application of Modified Algorithm to YADH

In recent work, the rate algorithm with CMD was applied to the calculation of the primary H/D KIE in YADH (Varga & Schwartz, 2016). This is the first application of the Chandler rate algorithm to an enzyme, as well as the first application in tandem with CMD. These simulations required the generation of more than 20,000 trajectories of which approximately 1800 were accepted. As mentioned previously, calculation of the first term proceeds via a normal TPS simulation. Reactive trajectories populated a cumulative histogram of $\langle h_p(t) \rangle$ (Fig. 2).

From this, one can see the linear region formed around 800 timesteps, or 400 fs. This linear region, when fit to a linear regression, yielded a slope corresponding to the value of the first term, $9.901 \times 10^{-4}\ \text{fs}^{-1}$ and $1.033 \times 10^{-3}\ \text{fs}^{-1}$ for the hydride and deuteride systems, respectively. Second term computations started from a trajectory from the first term calculation as a starting trajectory. Each system's trajectory was split into multiple windows based on order parameter, 7 for the hydride system and 9 for the deuteride system (Tables 3 and 4).

As can be seen in Table 3, windows 4 and 5 were difficult to populate with trajectories, with acceptance ratios of less than 5%. Similarly, windows 5, 6, 7, and 8 were difficult to populate in the deuteride system (Table 4).

This is likely because these windows lay on or around the free energy barrier, making it unlikely for the system to linger in those windows. Fig. 3 shows the completed and normalized histograms, with Hermite interpolated fits, and the product regions of the histograms with their fits. The second term value of the full rate equation is then calculated through integration of the product region fits. Combined with the first term values, we obtained a calculated primary H/D KIE of 5.22 for the conversion of benzyl alcohol to benzaldehyde in YADH.

As discussed earlier, the primary H/D KIE for the conversion of benzyl alcohol to benzaldehyde in YADH is 3.4, determined through non-competitive KIE studies (Klinman, 1976). The calculated result is within the margin of error of the experimentally determined result. Due to the nature of these experimental studies, the KIE is determined from the Michaelis complex to the first irreversible step (Simon & Palm, 1966),

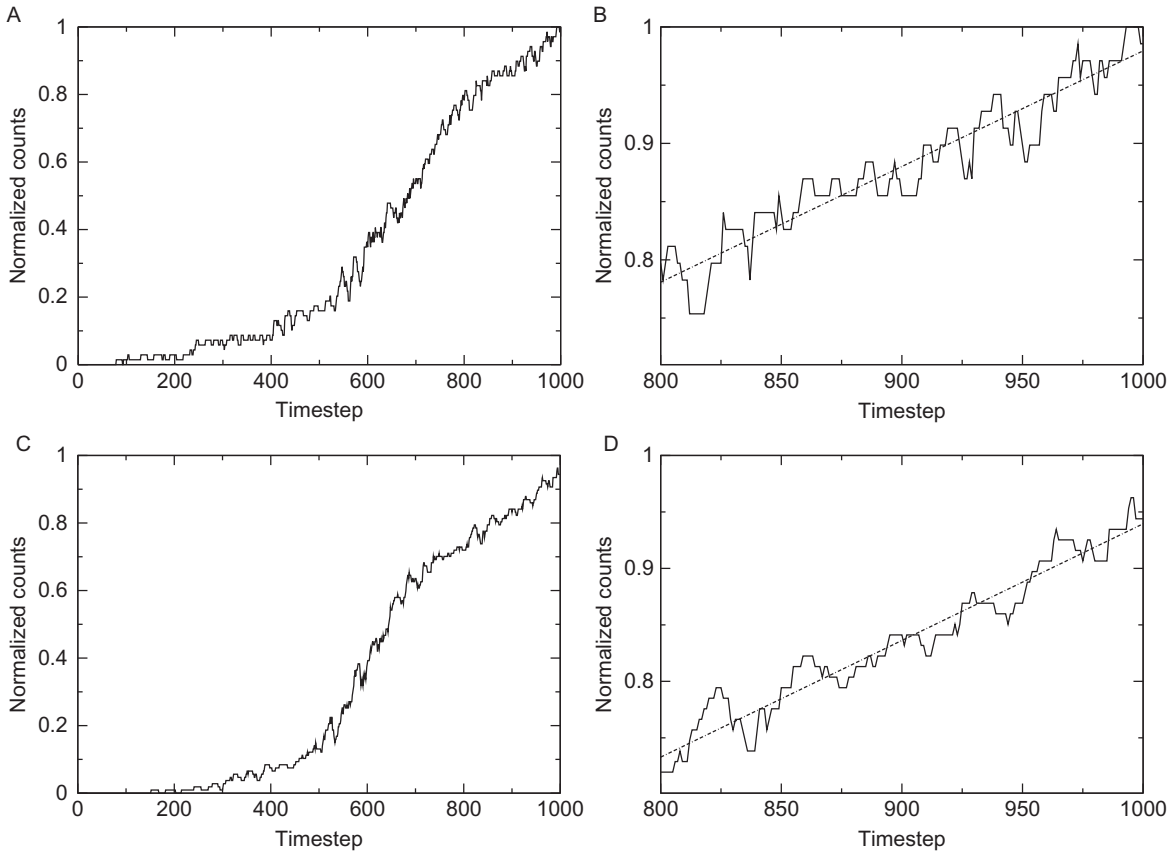

Fig. 2 Cumulative histograms for the calculation of the first term for hydride (A) and deuteride (C) systems, normalized to unity integral. Fits of the linear region, from 800 to 1000 timesteps (400–500 fs) are shown in *dashed lines* for hydride (B) and deuteride (D) systems. The slope of these linear fits are the values for the first term of the rate calculation.

Table 3 Windows and Their Member Trajectories for the Calculation of $C(t')$ in the Hydride system

Window	Range of Order Parameter (λ)	Accepted Trajectories	Total Trajectories	Acceptance Ratio (%)
1	0.200–0.360	216	493	43.8
2	0.350–0.410	179	487	36.8
3	0.400–0.460	167	1087	15.4
4	0.450–0.510	68	2066	3.10
5	0.500–0.560	56	2072	2.70
6	0.550–0.610	111	1303	8.51
7	0.600–0.900	125	811	15.4

Note the low acceptance ratio near the barrier, in windows 4, 5, and 6.

Table 4 Windows and Their Member Trajectories for the Calculation of $C(t')$ in the Deuteride System

Window	Range of Order Parameter (λ)	Accepted Trajectories	Total Trajectories	Acceptance Ratio (%)
1	0.170–0.260	201	517	38.9
2	0.250–0.310	150	506	29.6
3	0.300–0.350	113	481	23.5
4	0.350–0.400	138	744	18.5
5	0.400–0.450	40	885	4.52
6	0.450–0.510	46	2513	1.83
7	0.500–0.560	59	2451	2.35
8	0.550–0.610	94	2630	3.57
9	0.600–0.900	101	1458	6.9

Note the low acceptance ratio near the barrier, in windows 5, 6, 7, and 8.

the transition state in the case of YADH (Klinman, 1976). In an enzymatic reaction, a conformational search occurs to reach a reactive conformation from the Michaelis complex. However, the timescales of TPS trajectories require the simulation to start at or near the reactive conformation, excluding this conformational search. This extra step included in the experimental studies has the ability to mask a larger KIE on the transfer event alone, in the case where the conformational search is not affected by isotopic substitution (Schramm, 2011).

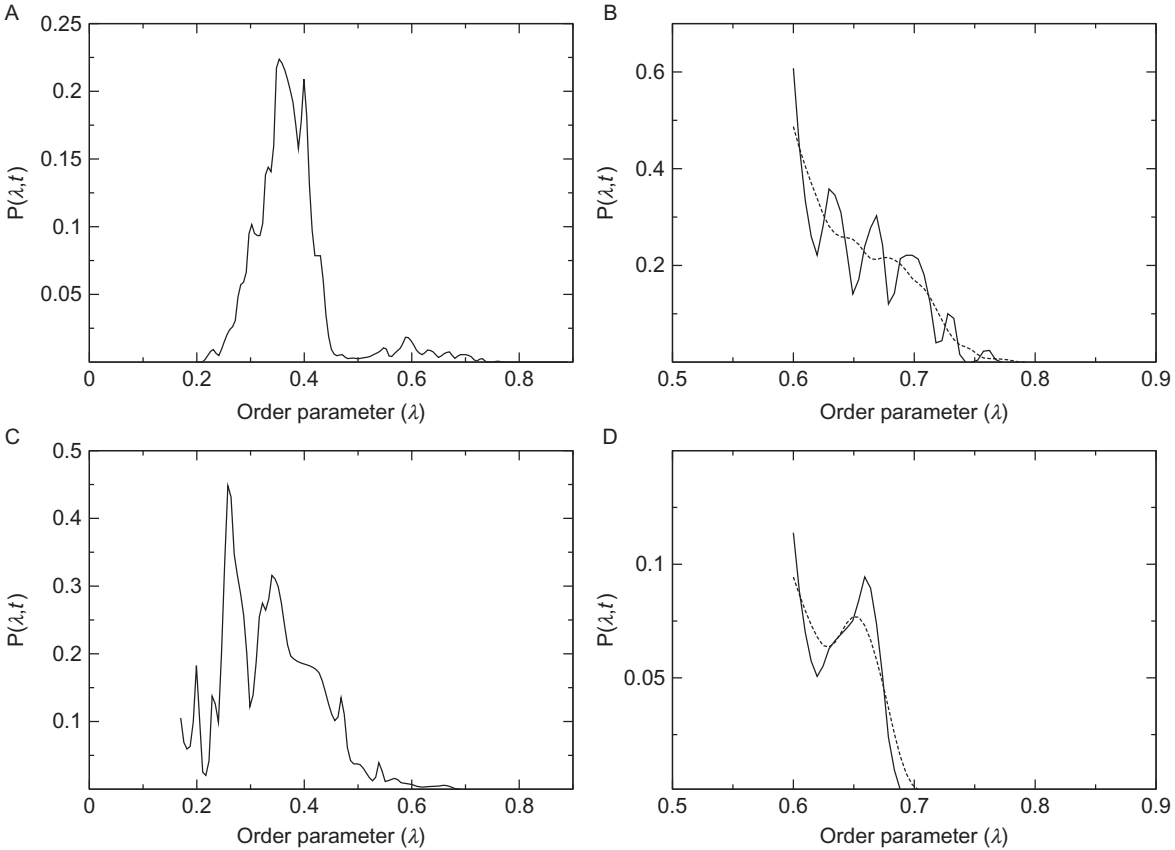

Fig. 3 Normalized histograms depicting the Hermite interpolation of full distribution function, $P(\lambda, t)$, for the calculation of $C(t')$ for the hydride (A) and deuteride (C) systems. The last window, $P(\lambda, t; i)$, of each distribution ((B) for the hydride system and (D) for the deuteride system) was denoted as the product region and was smoothed with a Gaussian function (shown in the *dashed line*) which was then integrated to determine $C(t')$.

4. CONCLUSION

We have summarized newly developed methods which combine a first principles sampling method, TPS, with quantum propagation of transferring particles, CMD. These methods were successfully applied to the calculation of free energy barriers in YADH and LDH and the primary H/D KIE in LDH. The inclusion of full protein and quantum dynamics into the calculation of free energy barriers and KIEs is a crucial stepping stone toward a more refined computational view of enzymatic mechanism.

REFERENCES

Amadei, A., Linssen, A. B. M., & Berendsen, H. J. C. (1993). Essential dynamics of proteins. *Proteins*, *17*, 412–425.

Antoniou, D., Ge, X., Schramm, V. L., & Schwartz, S. D. (2012). Mass modulation of protein dynamics associated with barrier crossing in purine nucleoside phosphorylase. *Journal of Physical Chemistry Letters*, *3*, 3538–3555.

Antoniou, D., & Schwartz, S. D. (2009). Approximate inclusion of quantum effects in transition path sampling. *The Journal of Chemical Physics*, *131*(22), 224111.

Basner, J. E., & Schwartz, S. D. (2005). How enzyme dynamics helps catalyze a reaction in atomic detail: A transition path sampling study. *Journal of the American Chemical Society*, *127*(40), 13822–13831.

Bennett, C. H. (1977). Molecular dynamics and transition state theory: the simulation of infrequent events. In R. E. Christofferson (Ed.), *ACS symposium series*: *Vol. 46. Algorithms for chemical computations* (pp. 63–97). Washington, DC: American Chemical Society.

Bolhuis, P. G., Chandler, D., Dellago, C., & Geissler, P. L. (2002). Transition path sampling: Throwing ropes over rough mountain passes, in the dark. *Annual Review of Physical Chemistry*, *53*(1), 291–318.

Bolhuis, P. G., Dellago, C., & Chandler, D. (1998). Sampling ensembles of deterministic transition pathways. *Faraday Discussions*, *110*, 421–436.

Brooks, B. R., Brooks, C. L., Mackerell, A. D., Nilsson, L., Petrella, R. J., Roux, B., … Karplus, M. (2009). CHARMM: The biomolecular simulation program. *Journal of Computational Chemistry*, *30*(10), 1545–1614.

Brooks, B. R., Bruccoleri, R. E., Olafson, B. D., States, D. J., Swaminathan, S., & Karplus, M. (1983). CHARMM: A program for macromolecular energy, minimization, and dynamics calculations. *Journal of Computational Chemistry*, *4*(2), 187–217.

Brothers, E. N., Suarez, D., Deerfield, D. W., & Merz, K. M. (2004). PM3-compatible zinc parameters optimized for metalloenzyme active sites. *Journal of Computational Chemistry*, *25*(14), 1677–1692.

Cao, J., & Voth, G. A. (1994a). The formulation of quantum statistical mechanics based on the Feynman path centroid density. I. Equilibrium properties. *The Journal of Chemical Physics*, *100*(7), 5093–5104.

Cao, J., & Voth, G. A. (1994b). The formulation of quantum statistical mechanics based on the Feynman path centroid density. II. Dynamical properties. *The Journal of Chemical Physics*, *100*(7), 5106–5117.

Cao, J., & Voth, G. A. (1994c). The formulation of quantum statistical mechanics based on the Feynman path centroid density. III. Phase space formalism and analysis of centroid molecular dynamics. *The Journal of Chemical Physics*, *101*(7), 6157–6167.

Cao, J., & Voth, G. A. (1994d). The formulation of quantum statistical mechanics based on the Feynman path centroid density. IV. Algorithms for centroid molecular dynamics. *The Journal of Chemical Physics*, *101*(7), 6168–6183.

Cao, J., & Voth, G. A. (1994e). The formulation of quantum statistical mechanics based on the Feynman path centroid density. V. Quantum instantaneous normal mode theory of liquids. *The Journal of Chemical Physics*, *101*(7), 6184–6192.

Cha, Y., Murray, C. J., & Klinman, J. P. (1989). Hydrogen tunneling in enzyme reactions. *Science*, *243*(4896), 1325–1330.

Chandler, D. (1978). Statistical mechanics of isomerization dynamics in liquids and the transition state approximation. *The Journal of Chemical Physics*, *68*, 2959.

Ciccotti, G., Kapral, R., & Vanden-Eijnden, E. (2005). Blue moon sampling, vectorial reaction coordinates, and unbiased constrained dynamics. *ChemPhysChem*, *6*(9), 1809–1814.

Cook, P. F., & Cleland, W. W. (2007). *Enzyme kinetics and mechanism*. New York City: Taylor & Francis.

Crehuet, R., & Field, M. J. (2007). A transition path sampling study of the reaction catalyzed by the enzyme chorismate mutase. *The Journal of Physical Chemistry. B*, *111*(20), 5708–5718.

Dellago, C., Bolhuis, P. G., & Chandler, D. (1998a). Efficient transition path sampling: Application to Lennard-Jones cluster rearrangements. *The Journal of Chemical Physics*, *108*(22), 9236–9245.

Dellago, C., Bolhuis, P. G., & Chandler, D. (1999). On the calculation of reaction rate constants in the transition path ensemble. *The Journal of Chemical Physics*, *110*(14), 6617–6625.

Dellago, C., Bolhuis, P. G., Csajka, F. S., & Chandler, D. (1998b). Transition path sampling and the calculation of rate constants. *The Journal of Chemical Physics*, *108*(5), 1964–1977.

Dzierlenga, M. W., Antoniou, D., & Schwartz, S. D. (2015). Another look at the mechanisms of hydride transfer enzymes with quantum and classical transition path sampling. *The Journal of Physical Chemistry Letters*, *6*(7), 1177–1181.

Ganzhorn, A. J., Green, D. W., Hershey, A. D., Gould, R. M., & Plapp, B. V. (1987). Kinetic characterization of yeast alcohol dehydrogenases. Amino acid residue 294 and substrate specificity. *The Journal of Biological Chemistry*, *262*(8), 3754–3761.

Gao, J., Amara, P., Alhambra, C., & Field, M. J. (1998). A generalized hybrid orbital (GHO) method for the treatment of boundary atoms in combined QM/MM calculations. *The Journal of Physical Chemistry. A*, *102*(24), 4714–4721.

Hayes, J. E., & Velick, S. F. (1954). Yeast alcohol dehydrogenase: Molecular weight, coenzyme binding, and reaction equilibria. *The Journal of Biological Chemistry*, *207*(2), 225–244.

Horiuti, J. (1938). On the statistical mechanical treatment of the absolute rate of chemical reaction. *Bulletin of the Chemical Society of Japan*, *13*(1), 210–216.

Hynes, J. T. (1985). Chemical reaction dynamics in solution. *Annual Review of Physical Chemistry*, *36*, 573–597.

Jarzynski, C. (1997). Nonequilibrium equality for free energy differences. *Physical Review Letters*, *78*(14), 2690–2693.

Kästner, J. (2011). Umbrella sampling. *Wiley Interdisciplinary Reviews: Computational Molecular Science*, *1*(6), 932–942.

Kästner, J., & Thiel, W. (2005). Bridging the gap between thermodynamic integration and umbrella sampling provides a novel analysis method: "Umbrella integration" *The Journal of Chemical Physics*, *123*(14), 144104.

Kipp, D. R., Silva, R. G., & Schramm, V. L. (2011). Mass-dependent bond vibrational dynamics influence catalysis by HIV-1 protease. *Journal of the American Chemical Society*, *133*(48), 19358–19361.

Kirkwood, J. G. (1935). Statistical mechanics of fluid mixtures. *The Journal of Chemical Physics*, *3*(1935), 300–313.
Kirkwood, J. G. (1936). Statistical mechanics of liquid solutions. *Chemical Reviews*, *19*(3), 275–307.
Klinman, J. P. (1972). The mechanism of enzyme-catalyzed reduced nicotinamide adenine dinucleotide-dependent reductions. Substituent and isotope effects in the yeast alcohol dehydrogenase reaction. *The Journal of Biological Chemistry*, *247*(24), 7977–7987.
Klinman, J. P. (1976). Isotope effects and structure-reactivity correlations in the yeast alcohol dehydrogenase reaction. A study of the enzyme-catalyzed oxidation of aromatic alcohols. *Biochemistry*, *15*(9), 2018–2026.
Klinman, J. P. (2009). An integrated model for enzyme catalysis emerges from studies of hydrogen tunneling. *Chemical Physics Letters*, *471*(4-6), 179–193.
Kumar, S., Rosenberg, J. M., Bouzida, D., Swendsen, R. H., & Kollman, P. A. (1992). The weighted histogram analysis method for free-energy calculations on biomolecules. I. The method. *Journal of Computational Chemistry*, *13*(8), 1011–1021.
Layfield, J. P., & Hammes-Schiffer, S. (2014). Hydrogen tunneling in enzymes and biomimetic models. *Chemical Reviews*, *114*(7), 3466–3494.
Machleder, S. Q., Pineda, J. R. E. T., & Schwartz, S. D. (2010). On the origin of the chemical barrier and tunneling in enzymes. *Journal of Physical Organic Chemistry*, *23*(7), 690–695.
Major, D. T., & Gao, J. (2007). An integrated path integral and free-energy perturbation—Umbrella sampling method for computing kinetic isotope effects of chemical reactions in solution and in enzymes. *Journal of Chemical Theory and Computation*, *3*, 949–960.
Masterson, J. E., & Schwartz, S. D. (2013). Changes in protein architecture and subpicosecond protein dynamics impact the reaction catalyzed by lactate dehydrogenase. *The Journal of Physical Chemistry. A*, *117*(32), 7107–7113.
Masterson, J. E., & Schwartz, S. D. (2014). The enzymatic reaction catalyzed by lactate dehydrogenase exhibits one dominant reaction path. *Chemical Physics*, *442*(17), 132–136.
Onsager, L. (1933). Theories of concentrated electrolytes. *Chemical Reviews*, *13*(1), 73–89.
Onsager, L. (1938). Initial recombination of ions. *Physical Review*, *54*(8), 554–557.
Park, S., & Schulten, K. (2004). Calculating potentials of mean force from steered molecular dynamics simulations. *The Journal of Chemical Physics*, *120*(13), 5946.
Quaytman, S. L., & Schwartz, S. D. (2007). Reaction coordinate of an enzymatic reaction revealed by transition path sampling. *Proceedings of the National Academy of Sciences of the United States of America*, *104*(30), 12253–12258.
Roston, D., & Kohen, A. (2013). A critical test of the "tunneling and coupled motion" concept in enzymatic alcohol oxidation. *Journal of the American Chemical Society*, *135*(37), 13624–13627.
Saunders, W. H., Jr. (1985). Calculations of isotope effects in elimination reactions. New experimental criteria for tunneling in slow proton transfers. *Journal of the American Chemical Society*, *107*(1), 164–169.
Schramm, V. L. (2011). Enzymatic transition states, transition-state analogs, dynamics, thermodynamics, and lifetimes. *Annual Review of Biochemistry*, *80*, 703–732.
Silva, R. G., Murkin, A. S., & Schramm, V. L. (2011). Femtosecond dynamics coupled to chemical barrier crossing in a Born-Oppenheimer enzyme. *Proceedings of the National Academy of Sciences of the United States of America*, *108*(46), 18661–18665.
Simon, H., & Palm, D. (1966). Isotope effects in organic chemistry and biochemistry. *Angewandte Chemie, International Edition*, *5*(11), 920–933.
Stewart, J. J. P. (1989a). Optimization of parameters for semiempirical methods I. Method. *Journal of Computational Chemistry*, *10*(2), 209–220.
Stewart, J. J. P. (1989b). Optimization of parameters for semiempirical methods II. Applications. *Journal of Computational Chemistry*, *10*(2), 221–264.

Straatsma, T. P., & Berendsen, H. J. C. (1988). Free energy of ionic hydration: Analysis of a thermodynamic integration technique to evaluate free energy differences by molecular dynamics simulations. *The Journal of Chemical Physics*, *89*(9), 5876.

Swain, C. G., Stivers, E. C., Reuwer, J. F., Jr., & Schaad, L. J. (1958). Use of hydrogen isotope effects to identify the attacking nucleophile in the enolization of ketones catalyzed by acetic acid. *Journal of the American Chemical Society*, *80*(21), 5885–5893.

Torrie, G. M., & Valleau, J. P. (1977). Nonphysical sampling distributions in Monte Carlo free-energy estimation: Umbrella sampling. *Journal of Computational Physics*, *23*(2), 187–199.

Truhlar, D. G. (2010). Tunneling in enzymatic and nonenzymatic hydrogen transfer reactions. *Journal of Physical Organic Chemistry*, *23*(7), 660–676.

Vanden-Eijnden, E., & Tal, F. A. (2005). Transition state theory: Variational formulation, dynamical corrections, and error estimates. *The Journal of Chemical Physics*, *123*(18), 184103.

Varga, M. J., & Schwartz, S. D. (2016). Enzymatic kinetic isotope effects from first-principles path sampling calculations. *Journal of Chemical Theory and Computation*, *12*(4), 2047–2054.

Warshel, A., & Levitt, M. (1976). Theoretical studies of enzymic reactions: Dielectric, electrostatic and steric stabilization of the carbonium ion in the reaction of lysozyme. *Journal of Molecular Biology*, *103*(2), 227–249.

Wick, C. D. (2009). NaCl dissociation dynamics at the air–water interface. *The Journal of Physical Chemistry. C*, *113*(6), 2497–2502.

Wick, C. D., & Dang, L. X. (2010). Computational investigation of the influence of organic-aqueous interfaces on NaCl dissociation dynamics. *The Journal of Chemical Physics*, *132*(4), 044702.

Xia, F., Bronowska, A. K., Cheng, S., & Gräter, F. (2011). Base-catalyzed peptide hydrolysis is insensitive to mechanical stress. *The Journal of Physical Chemistry. B*, *115*(33), 10126–10132.

Zhang, Y., Liu, H., & Yang, W. (2000). Free energy calculation on enzyme reactions with an efficient iterative procedure to determine minimum energy paths on a combined *ab initio* QM/MM potential energy surface. *The Journal of Chemical Physics*, *112*(8), 3483–3492.